Iran University of Science and Technology

Automotive Science and Engineering

Journal Homepage: ijae.iust.ac.ir

ISSN: 2008-9899

Numerical study of hydrogen addition impact on combustion characteristics of a natural gas fueled Engine

Fereshteh Khodamrezaee[1], Ali Keshavarz*[1] , Sadegh Seddighi[1], Sepide Sarmast

[1] Mechanical engineering faculty, K. N. Toosi University of Technology, Tehran, Iran

ARTICLE INFO

Article history:

Received : 20 Jan 2018

Accepted: 29 May 2020

Published: 01 Dec 2020

Keywords:

Spark Ignition (SI) Engine, Hydrogen, Compressed Natural Gas (CNG), Carbon Monoxide, Emission.

A B S T R A C T

This work investigates the effects of hydrogen addition to compressed natural gas (CNG) on combustion characteristics and emission reduction using a closed cycle simulation with exact geometry of piston and cylinder head. The effect of equivalence ratio on combustion characteristic were investigated using a spark ignition (SI) engine fueled with CNG and addition of 10% vol, 15% vol and 20%vol hydrogen. Two different speed of 1500 and 3000 rpm have considered at full load condition. The modeling includes ECFM combustion model combined with K-ζ-f turbulent model and has been done by AVL Fire software. Different volume fraction of Hydrogen with different excess air modeled and validated with experimental data. The validation procedure included in-cylinder pressure profile, maximum pressure, angle of maximum pressure, indicated mean effective pressure, and carbon monoxide (CO) emission showing a good agreement with the experimental results. The value of the peak pressure increases by hydrogen addition and it takes place sooner as the hydrogen volume fraction increases. However, the mean effective pressure drops 3.5%, 7% and 15% for HCNG 10, HCNG15 and HCNG20, respectively. CO emission decreases by increasing the hydrogen volume fraction. The results also indicate that hydrogen addition in lean combustion causes more CO reduction compared to the fuel-rich mixtures.

1 Introduction

Experimental studies show that the addition of small amounts of hydrogen to CNG makes the fuel cleaner and provides faster rate of burning than CNG alone [1,2]. Specifically, hydrogen addition to CNG reduces emissions such as unburned hydrocarbons (UHC), CO and CO2, while having a tendency to increase NOx emissions. However, a fuel-leaner combustion compared to typical conditions can be achieved

* **Ali Keshavarz**

Email Address: Keshavarz@kntu.ac.ir

https://doi.org/10.22068/ase.2020.529

[DOI: 10.22068/ase.2020.529]

with the hydrogen addition and results lower NOx emissions.

Wallace and Cattelan [3] experimentally studied emissions of an engine fueled with a mixture of natural gas and 15% hydrogen in a 3.1 Chevrolet Lumina with compression ratio of 8.8. Their results showed that the brake specific fuel consumption (BSFC) of the engine with 15% H2 addition is lower than CNG alone while NOx emission increases with hydrogen addition.

Raman et al. [4] reported that hydrogen is a useful additive for natural gas, enabling leaner operation under part load conditions and improving BMEP at full load operation. Moreover, they found that hydrogen addition leads to that NOx values are reduced while other emissions and fuel consumption does not change significantly compared to burning CNG alone.

Hoekstra et al. [5, 6] carried out experiments on a 17 hp SI engine at 1700 rpm with varying CNG/H2 ratios and different equivalence ratios measuring NOx and other emissions. They found that increasing equivalence ratios lead to NOx increase and unburned hydrocarbon (UHC) decrease. They found low NOx value at $\varphi = 0.625$ for 28 and 36 percent H2 volume fraction.

Paul et al. [7] studied the effect of hydrogen and CNG mixtures on emissions in an IC engines. They reported that increasing hydrogen volume fraction up to 30% resulted CO emission reduction about 55% at part load and 40% at full load condition. However at high load conditions and constant equivalence ratio NOX emissions increase with hydrogen addition. In addition, by increasing hydrogen up to 30% the efficiency of the engine increases about 80%.

Das [8] surveyed utilization of hydrogen and natural gas mixtures in an internal combustion engine. He clarified that hydrogen blended with CNG enabled leaner operation under part load conditions and showed an improvement in BMEP.

Dieguez et al [9] experimentally studied the engine performance and emissions of a SI engine fueled with methane-hydrogen mixture (5-20 vol% methane).They studied various fuel composition , air to fuel (AF) ratios , engine speed and spark timing. Their results show that air to fuel ratio have considerable impact on CO emission. For example CO emission at λ=2.5 is about 7 times higher than CO emission at λ=1.6. In addition, the emission reduction with engine speed increase reported due to the mixture mixing and turbulence improvement in cylinder flow.

Karim et al. [10] studied experimentally HCNG with different H2 volume fraction and varying equivalence ratios. They investigated flame initiation speed, power output differences, efficiency, average ignition lag, average combustion duration, average maximum cylinder pressure, knocking regions in different mixtures, different equivalence ratio and different BTDC. For 10 and 20 BTDC, with increasing concentration of hydrogen in the engine, power output increased, but for 30 BTDC, with the increasing concentration of hydrogen, power output decreased. The maximum power output has been shown to be at 20 BTDC. They also reported that by addition of hydrogen to the methane, performance characteristics of the engine increased drastically.

Lim et al. [11] considered retarding the ignition timing for an HCNG engine along with the compression ratio enhancement at maximum power operation. Emission characteristics and efficiency, investigated by retarding the ignition timing. The test conditions of HCNG30 are 11.5 compression ratio, 1.8 lambda, and 10 CAD retarding the ignition timing. The thermal efficiency increases 2.0%, NOx emission reduces 61.7%, and CH4 emission enhances 6.7% in comparison to CNG fuel.

Das et al. [12] investigated the thermal efficiency and BSFC of CNG and hydrogen mixture as fuel in an internal combustion engine. They reported that the BSFC reduced and the BTE improved with hydrogen operation compared to systems running on CNG alone. The BTE was as high as 31.19% for hydrogen operation compared to that of 27.59% for CNG.

Shudo et al. [13] investigated combustion and emissions of methane and hydrogen mixture fuel. They performed the test on a four-stroke cycle single cylinder SI engine with a bore × stroke of 85×88 mm and a CR of 13.They reported that thermal efficiency increased with hydrogen addition while unburned hydrocarbon decreased. NOx emissions tended to increase with hydrogen addition. However, this increase could be maintained at lower levels with retarded ignition timing.

[DOI: 10.22068/ase.2020.529]

Bauer et al. [14] studied the effect of hydrogen addition to the performance of methane-fueled engine. They used a one-cylinder research engine with compression ratio of 8.5. Brake power, ignition timing, BSFC, BSCO2, BSCO, BSHC, BSNO in different CH4/H2 mixture, different ER, load and speed has been investigated. They reported that hydrogen addition up to 60% volume resulted a decrease in BSCO2 up to 26% (from φ=0.58 to 1.0), in BSCO up to 40 %(for φ>0.95) in BSHC up to 60% (from φ=0.58 to 1.0), but an increase in peak BSNO at φ = 0.83 of approximately 30% (for volumetric fraction =40%).

Paul et al. [15] studied the effect of hydrogen/natural gas blends on emissions in lean-burn IC engines. They concluded that increasing hydrogen concentration from zero to 30% resulted in 55% reduction in CO emissions at part load and 40% at full load. The NOx emissions did not change significantly in part-load operation, while it was significant in high load conditions at fixed equivalence ratio. However, the rate of thermal efficiency decreases about 8% as hydrogen addition increases up to 30%. However, impacts of hydrogen addition on thermal efficiency was not significant at full load condition.

Shrestha et al. [16] investigated the impact of adding hydrogen to methane-fueled spark ignition internal combustion engines. The addition of hydrogen to methane increased performance, particularly during operation with lean mixtures at low equivalence ratios. Adding more than 20% hydrogen by volume adversely affected power output and led to increased knock.

Heffel [17] investigated the benefits of EGR on hydrogen-fueled engines over a variety of engine speeds. He reported that EGR with the use of a three-way catalytic converter is an effective means to reduce NOX emissions from hydrogen-fueled engines to less than 1 ppm.

As seen most of the above studies were performed experimentally and reported to some extent inconsistent results for different engines. One can conclude that various engine parameters such as engine geometry, excess air ratio, spark timing, and hydrogen addition are affecting the engine output and emissions. Hence, each engine has to be investigated individually to obtain the impact of hydrogen addition on the performance and emissions of that engine. In the current study, a comprehensive numerical study along with some experimental work was conducted to investigate the impact of hydrogen addition on a four-cylinder SI engine. The main goals of this study can be summarized as follows:

1. CFD simulation of CNG and HCNG15 fuel in an SI engine with exact geometry in different engine speeds and different excess air ratio.
2. Considering the proper turbulence and combustion modeling methodology for hydrogen-CNG combustion mixture.
3. Comparison combustion parameters for of CNG and HCNG fuels.

2 Modeling

The modeling in this work includes the intake valve opening (IVO), intake valve closing (IVC), spark timing, end of combustion (EOC), and exhaust valve opening (EVO). CNG inlet boundary condition is based on experiment and set to 325K and 100Kpa while HCNG condition is 315K and 100Kpa.

In experiment, to generate the mixture of HCNG15, hydrogen has been charged to the cylinder until the pressure of it reached the calculated partial pressure and then CNG was charged to the cylinder. The final temperature of HCNG15 was 315 K.

The calculations are carried out using an Intel Corei7 e 4790 K CPU @ 3.60 GHz Processor and 16 GB RAM in a 64-bit Operating System.

The engine is four stroke, spark ignition and naturally aspirated with 78.6 mm bore, 85 mm stroke, and compression ratio of 11 with four valves for each cylinder. The calculations are conducted at full load condition and different engine speeds of 1500, 3000 rpm. The equivalence ratios of CNG-hydrogen-air mixtures are 0.6, 0.7, 0.8, 0.9 and 1. The spark timing is changed based on the experimental data for all cases. Three different hydrogen volume fraction 10 %vol ،15 %vol and 20 %vol have been considered.

A compressible turbulent and chemically reacting flow with Reynolds average formulation is considered. Angled brackets (<>) denotes averaged mean quantities. The tildes (~) denotes Favre averaged mean quantities. The following governing equations, continuity, momentum,

[DOI: 10.22068/ase.2020.529]

energy and, species, respectively, are used in this simulation.[18].

$$\frac{\partial^2\langle P\rangle}{\partial x_i x_i} = \frac{\partial^2\langle\rho\rangle}{\partial t^2} - \frac{\partial^2\langle\rho\rangle\tilde{u}_i\tilde{u}_j}{\delta x_i \delta x_j} + \frac{\partial^2(\langle\tau_{ij}\rangle + \tau_{T,ij})}{\delta x_i \delta x_j} + g_j\frac{\partial\langle\rho\rangle}{\partial x_j} \quad (1)$$

$$\frac{\partial\langle\rho\rangle\tilde{u}_j}{\partial t} + \frac{\partial\langle\rho\rangle\tilde{u}_j\tilde{u}_i}{\partial x_i} = \frac{\partial(\langle\tau_{ij}\rangle + \tau_{T,ij}}{\partial x_i x_j} - \frac{\partial\langle P\rangle}{\partial x_j} + \langle\rho\rangle g_j \quad (2)$$

$$\frac{\partial\langle\rho\rangle\tilde{h}}{\partial t} + \frac{\partial\langle\rho\rangle\tilde{h}\tilde{u}_i}{\partial x_i} = \frac{\partial}{\partial x_i}\left[(\frac{\lambda}{C_P} + \frac{\mu_T}{Pr_T})\frac{\partial\tilde{h}}{\partial x_i}\right] + \frac{\partial\langle P\rangle}{\partial t} + \tilde{u}_i\frac{\partial\langle P\rangle}{\partial x_i} + \Phi \quad (3)$$

$$\frac{\partial\langle\rho\rangle\tilde{Y}_\alpha}{\partial t} + \frac{\partial\langle\rho\rangle\tilde{Y}_\alpha\tilde{u}_i}{\partial x_i} = \frac{\partial}{\partial x_i}\left[\left(\frac{\mu}{Sc_\alpha} + \frac{\mu_T}{Sc_{T,\alpha}}\right)\frac{\partial\tilde{Y}_\alpha}{\partial x_i}\right] + \langle\rho\rangle\tilde{S}_\alpha \quad (4)$$

$$\Phi = \langle\tau_{ij}\rangle\frac{\partial\tilde{u}_i}{\partial x_j} + \langle\rho\rangle\varepsilon \quad (5)$$

Where u_i is a velocity component , P is pressure , ρ is density , g is constant body force per unit mass, h is enthalpy , Y is mass fraction, α is chemical species, μ and μ_T are molecular viscosity and apparent turbulent viscosity, respectively. Φ is viscous dissipation rate, S is mass based chemical source term, C_p is constant pressure specific –heat capacity. The viscous shear stress is τ_{ij} , τ_{Tij} is an apparent turbulent stress. Pr_T and $Sc_{T,\alpha}$ are apparent turbulent prandtl and Schmidt numbers, respectively.

Turbulence modeling:

To predict the turbulent effect, the method of averaging the governing equations of the flow (RANS) utilized, which is proper for large-scale industrial engines. The non-linearity of the Navier- Stokes equations appears in the RANS equations is Reynolds stress ($-\rho\overline{v_i'v_j'}$).The k-ε-ζ-f model, which is a four- equation model, utilized by [19, 20, 21], are utilized to calculate the Reynolds stress.

The k-ε-ζ-f In comparison with the k-ε turbulence model, as its formulation shows, demonstrates more capability to capture the different near wall effect (the damping effects of viscosity and pressure reflection) in turbulence flows.
These four equations are:
Turbulent kinetic energy (K):

$$\frac{\partial\rho k}{\partial t} + \frac{\partial(\rho u_j k)}{\partial x_j} = P - \rho\varepsilon + \frac{\partial}{\partial x_j}[\left(\mu + \frac{\mu_l}{\sigma_k}\right)\frac{\partial k}{\partial x_j}] \quad (6)$$

Turbulent kinetic energy dissipation rate (ε):

$$\frac{\partial\rho\varepsilon}{\partial t} + \frac{\partial(\rho u_j\varepsilon)}{\partial x_j} = \frac{C_{\varepsilon1}P - C_{\varepsilon2}\rho\varepsilon}{T} + \frac{\partial}{\partial x_j}[\left(\mu + \frac{\mu_l}{\sigma_\varepsilon}\right)\frac{\partial\varepsilon}{\partial x_j}] \quad (7)$$

Normalized velocity scale (ζ)

$$\frac{\partial\rho\zeta}{\partial t} + \frac{\partial(\rho u_j\zeta)}{\partial x_j} = \rho f - \frac{\zeta}{k}P + \frac{\partial}{\partial x_j}[\left(\mu + \frac{\mu_t}{\sigma_\zeta}\right)\frac{\partial\zeta}{\partial x_j}] \quad (8)$$

Non-locality is represented by an elliptic relaxation function for *f*:

[DOI: 10.22068/ase.2020.529]

$$L^2\nabla^2 f - f = L^2\frac{\partial}{\partial x_j}\left(\frac{\partial f}{\partial x_j}\right) - f = \frac{1}{T}(C_1 - 1 + C_2'\frac{P}{\rho\varepsilon})(\zeta - \frac{2}{3}) \quad (9)$$

Where, P is the production of the turbulent kinetic energy.

$$P = \tau_{ij}\frac{\partial u_i}{\partial x_j} \quad (10)$$

$$\tau_{ij} = \mu_t\left(2S_{ij} - \frac{2}{3}\frac{\partial u_k}{\partial x_k}\delta_{ij}\right) - \frac{2}{3}\rho k\delta_{ij} \quad (11)$$

$$S_{ij} = \frac{1}{2}(\frac{\partial u_i}{\partial x_j} + \frac{\partial u_j}{\partial x_i}) \quad (12)$$

For incompressible flows, the production term exactly becomes:

$$P = \mu_t S^2 \quad (13)$$

In addition, the Modulus of the mean rate-of-strain tensor is:

$$S = \sqrt{2S_{ij}S_{ij}} \quad (14)$$

The turbulent eddy viscosity is computed from:

$$\mu_t = \rho C_\mu \zeta k T \quad (15)$$

The turbulence time scale and length scale computed from:

$$T = \max[\min\left(\frac{k}{\varepsilon}, \frac{0.6}{\sqrt{6}C_\mu|S|\zeta}\right), C_T\left(\frac{\upsilon}{\varepsilon}\right)^{1/2}] \quad (16)$$

$$L = C_L\max[\min\left(\frac{k^{3/2}}{\varepsilon}, \frac{k^{1/2}}{\sqrt{6}C_\mu|S|\zeta}\right), C_\eta\left(\frac{\upsilon^3}{\varepsilon}\right.$$ (17)

Model coefficients:

$C_\mu = 0.22$ $\sigma_k = 1.0$ $\sigma_\varepsilon = 1.3$ $\sigma_\zeta = 1.2$ $C_{\varepsilon 1} = 1.4[1 + \left(\frac{0.012}{\zeta}\right)]$

$C_{\varepsilon 2} = 1.9$ $C_2' = 0.65$ $C_1 = 1.4$ $C_T = 6$ $C_L = 0.36$ $C_\eta = 85$

Combustion modeling:

The Extended Coherent Flame Model (ECFM) [22], which is suited for premixed flame combustion, used in this study. This model utilized due to its capability of modeling multi component fuels combustion. The ECFM is based on a flame surface density equation. This model considers the wrinkling of the flame front surface by turbulent eddies. A conditioning averaging technique allows precise reconstruction of local properties in fresh and burned gases.

The model describes the rate of fuel consumption per unit volume by product of flame surface density and local speed. The multi –component combustion model is based on the definition of a mean local fuel, which presents all the components of fuel.

Computational mesh:

The engine geometry has been used with cylinder head curvature and the inflate piston head. So the errors due to the combustion chamber simplification is minimized. Fig (2) shows the closed cylinder head along with spark plug and valves.

In this research, the combustion chamber moving mesh has been created with the maximum and minimum grid size of 2 and 0.5 mm. For creating moving mesh, the maximum grid length of 0.5 mm has been considered.

[DOI: 10.22068/ase.2020.529]

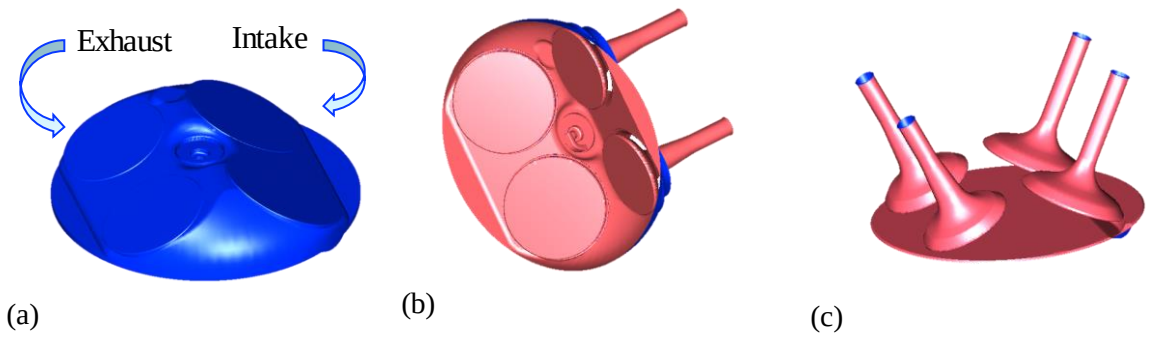

Figure 1. EF7 engine (a) Close cycle control volume, (b) Cylinder head and spark plug,(c) Piston and valve

Figure (3) illustrated the mesh generation in the state of IVC. As is shown in this figure, unstructured mesh are utilized in near wall and structured mesh are used for remaining volume. The maximum mesh number in BDC is bout 634000. To reduce the calculation time, the simulation has been carried out from IVO to EVC. Grid independency has been done to prevent the meshing size effects on the results and reduce the time of calculation. Different grids are created for mesh study in table 4. An assumption of the results indicates an almost negligible discrepancy between the results obtained from the first two cases 985000 and 634000 grids. Therefore, the case with 634000 grid is used.

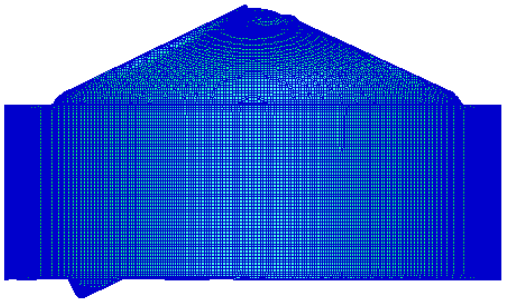

Figure 2. The solution domain and mesh generation at 660 crank angles

Table 1. The specification of used meshes for 1500 rpm – CNG and close cycle condition.

Grid NO.	Number of cells	Maximum Dimensions of chamber cells (mm)	Simulation time (h)	Max in-cylinder pressure (bar)
1	~985000	0.25	21	54
2	~634000	0.5	15	54
3	~369000	1	10	55
4	~276000	2	8	53

2.1 Calculation procedure:

2.2 Boundary and initial condition:

The boundary and initial conditions used in the numerical calculation are specified according to the experimental measurements as well as the reliable estimations. The initial pressure and temperature at IVC are obtained from the experimental measurement. The piston considered as a moving wall while the other walls are stationary. Appropriate profile is set for piston.

The time step in simulation has been set to 0.5CA for combustion and 1CA for the other process. The selected time step is small enough to provide time step independent solutions even for low engine speeds.

SIMPLE/PISO algorithm is utilize for pressure-velocity coupling. The PISO algorithm is found

[DOI: 10.22068/ase.2020.529]

to be efficient and fast in solving unsteady problems. The first order upwind differencing scheme is used for momentum, turbulence, energy and species equations. Convergence criteria for continuity, energy and species have been set to 10^{e-4}, 10^{e-7} and 10^{e-7}, respectively.

2.3 Experimental apparatus

Experiments carried out on a SI and naturally aspirated, four-cylinder engine. The engine specification provided in Table 1. It is four stroke, with bore, 78.6 mm, stroke, 85 mm, and compression ratio11. It has four valves per cylinder.

The engine runs at full load condition (WOT), stoichiometric condition and 1500 and 3000-rpm engine speed.

To generate the mixture HCNG15, hydrogen charged to the cylinder until the pressure of it reached the calculated partial pressure and then CNG charged to the cylinder up to 150 bar. The partial pressures of CNG and H_2 are 127.5 bar and 22.5 bar, respectively which were calculated by Dalton model. CNG and HCNG15 inlet temperatures were 325 and 315 K, respectively.

Fig 4 shows the schematic of experimental set up.

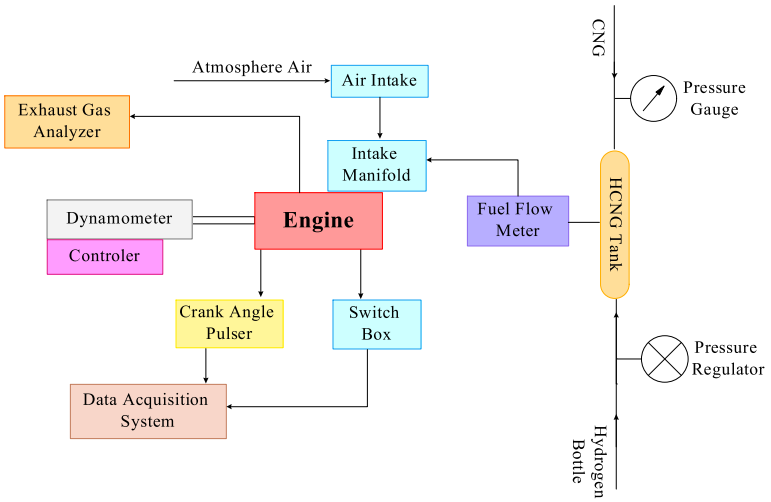

Figure 3. Experimental set up configuration

An eddy current dynamometer with the 230KW maximum power, 8500-rpm maximum speed and 800 N.M maximum torque utilized for engine speed and load measurements. The piso-electric sensors installed near the spark plugs for measuring instant cylinder pressure. Different kinds of thermocouples installed in the inlet and exhaust manifold .Angle encoder used to record the crank angle. The mixture of hydrogen and methane injected in the intake manifolds. A PC based data logger used to record all the measured values for 100 cycle. The recorded data consist of engine parameters, pressures, temperatures, fuel consumptions and emissions. Variations of pressure and the amount of fuel burning recorded at different crank angles.An in-house software calculated the optimum air - fuel ratio and ignition timing. The optimum spark timing is the time when the spark timing advanced or retarded until the mean effective pressure reached the theoretical value. The test carried out in stoichiometric condition.

3 Results and discussions

The effect of different volume fraction of hydrogen addition to CNG combustion in different equivalence ratio in the engine investigated. Closed cycle modeling with exact geometry of piston and cylinder head considered. The compression ratio kept constant and equal to 11.

The validation procedure also has been done for maximum pressure, angle of P_{max}, indicated mean effective pressure (IMEP) and CO emission, in each figure, separately. Comparison of The

[DOI: 10.22068/ase.2020.529]

simulation and experimental data provides a general view of the accuracy of the numerical results.

The most important in-cylinder combustion characteristics are considered in this section.

.

The maximum In-cylinder pressure with respect to different hydrogen volume fraction and equivalence ratio are shown in fig(5). Generally, maximum pressure increases with hydrogen addition, while it drops for lean burning. Also the maximum pressure enhances with engine speed.

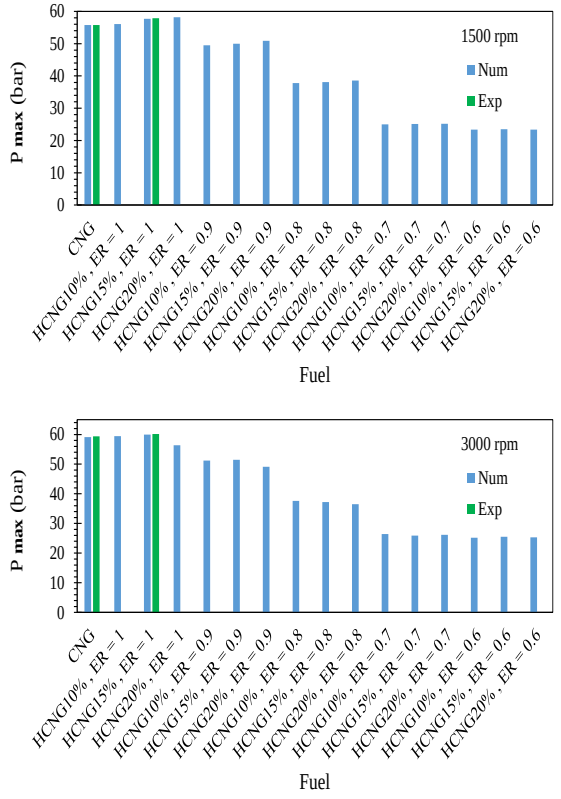

Figure 4. in-cylinder maximum pressure versus different hydrogen volume fraction and ER for a) 1500 rpm and b) 3000rpm.

The location of maximum pressure for different fuel mixture and different ER conditions illustrated in Fig 6. In section (a), it can be seen that maximum pressure takes place sooner as the hydrogen volume fraction increases. It can be concluded the combustion starting time can be retarded by adding hydrogen into the fuel mixture. In contrast, the combustion occurs faster when the excess air ratio increases for 1500 engine speed. Also, the angle of P_{max} occurs sooner at higher engine speed.

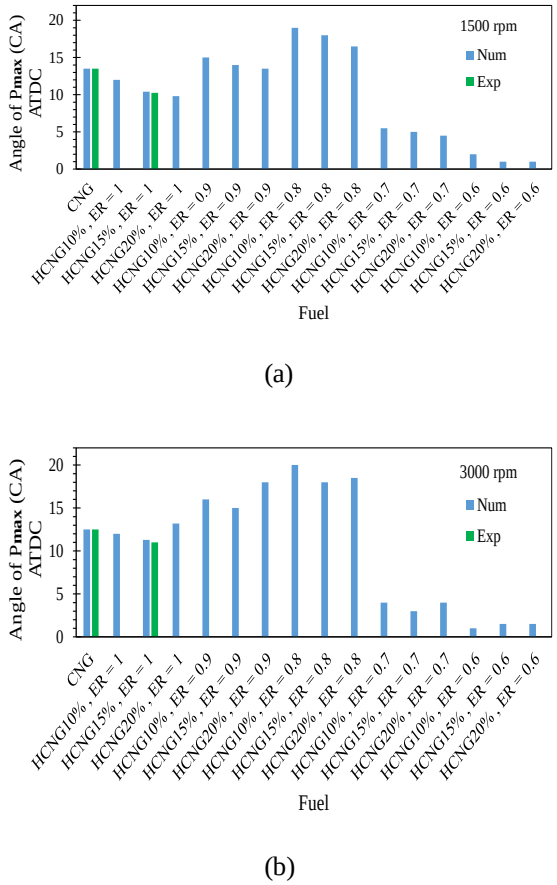

Figure 5. Angle of maximum pressure versus different hydrogen volume fraction and ER for a) 1500 rpm and b) 3000rpm.

Fig 7 shows indicated mean effective pressure (IMEP) at different Hydrogen volume fraction, different ER and different speeds. The general trend of mean effective pressure illustrate that increasing the AF ratio; have negative effect on engine power. The IMEP is higher in 3000 rpm engine speed.

[DOI: 10.22068/ase.2020.529]

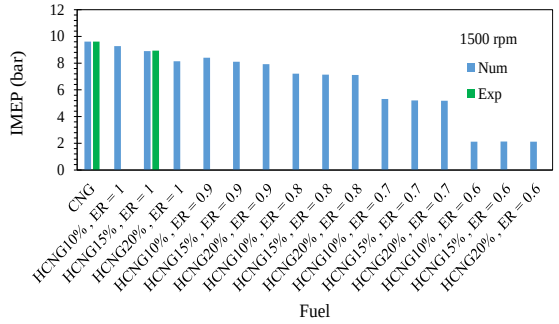

(a)

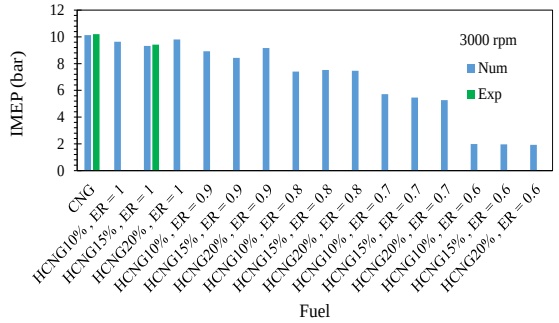

(b)

Figure 6. mean effective pressure versus different hydrogen volume fraction and ER for a) 1500 rpm and b) 3000rpm.

Fig (8) shows the in-cylinder pressure values in terms of the crank angle degree with different hydrogen volume fraction and stoichiometric condition .The value of the peak pressure increases by hydrogen addition and the highest pick pressure achieved in HCNG20. Maximum pressure of the HCNG increases in the same AF ratio, which enhances the tendency of self-ignition phenomena.

The mean effective pressure, which is defined as work divided by cylinder volume displacement per cycle, is a metric of engine work ability.

Figure 8 illustrate that mean effective pressure (MEP) of CNG drops by adding hydrogen. It is calculated 9.61 bar, 9.27 bar, 8.9 bar and 8.14 bar for CNG, HCNG10, HCNG15 and HCNG20, respectively.

It is because of low energy density of the hydrogen, which has negative impact on engine performance, especially in high content of hydrogen.

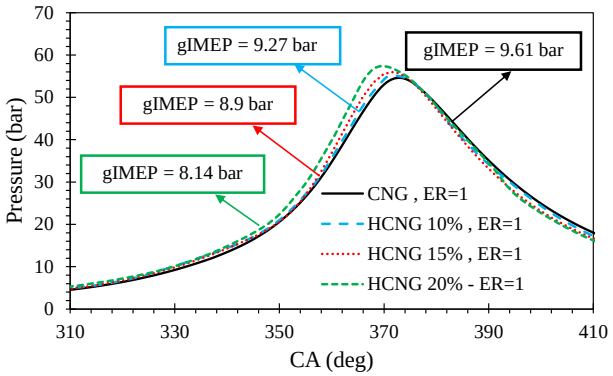

Figure 7. In-cylinder pressure versus crank angle degree for different hydrogen volume fraction, ER=1 and 1500 rpm

Fig (9) illustrates the CO emission values versus different hydrogen volume fraction and the excess air ratio. Its value decreased by increasing the hydrogen volume fraction and the excess air ratio. Lower carbon volume fraction, higher combustion duration and more uniform temperature profile could be the reasons of CO emission reduction .In addition, with more oxygen in lean burn condition, the possibility of CO_2 formation is higher than CO. In addition, carbon monoxide production is higher at 3000 rpm engine speed.

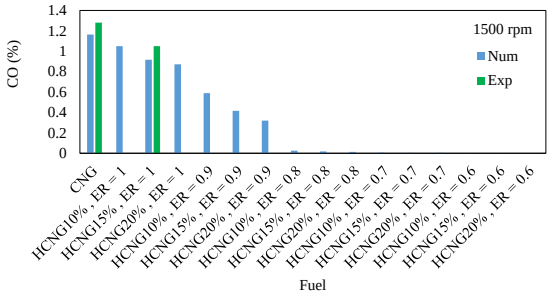

(a)

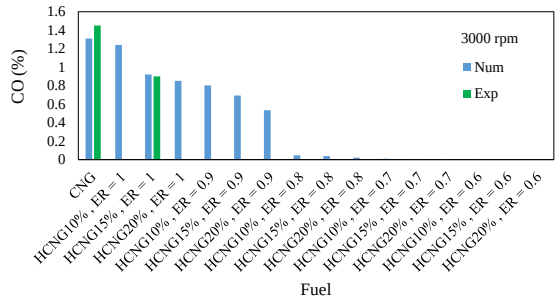

(b)

[DOI: 10.22068/ase.2020.529]

Figure 8. Computed and measured CO versus different hydrogen volume fraction and different excess air ratio.

4 Conclusion

In this, research the effect of Hydrogen addition into a CNG fueled engine is investigated numerically and experimentally.by focusing on the exhaust emission such as NOx and CO. Since the experiments was conducted ae ER=1 more numerical investigation was done for other ER and different speeds.

Some of the conclusion can be summarized as follows:

1) Maximum pressure of the CNG/H2 mixture increases by increasing hydrogen volume fraction at constant ER (about 3%). However, in lean burn combustion, its values drops. Also the maximum pressure, which is limiting parameter in engine design, enhances with engine speed.

2) Maximum pressure occurs sooner by H2 addition so the combustion starting time can be retarded. However, it should be advanced when the excess air ratio increases for 1500 engine speed. Also, the angle of Pmax occurs sooner at higher engine speed.

3) Hydrogen addition decreases the mean effective pressure of the engine due to its lower volumetric heating value. But it is negligible especially in lean burn condition. The IMEP is higher in 3000-rpm engine speed.

4) CO emission values decrease with increasing hydrogen volume fraction in stoichiometric and lean burn combustion.

It can be concluded that the hydrogen negative effects such as enhancing the maximum pressure and decreasing the engine mean effective pressure is negligible in lower engine speed. While it can decrease the emission and improve the flammability of CNG in this condition.

Nomenclatures

ATDC	After Top Dead Centre
BDC	Bottom Dead Centre
BTDC	Before Top Dead Centre
BMEP	Break Mean Effective Pressure
$BSCO_2$	Break specific CO_2
BSCO	Break Specific CO
BSFC	Break specific Fuel consumption
BSNO	Break Specific NO
BSHC	Break Specific Unburned Hydrocarbon
CA	Crank Angle degree
CR	Compression Ratio
CFD	Computational Fluid Dynamics
CNG	Compressed Natural Gas
HCNG	Hydrogen enriched Compressed Natural Gas
HCNG+ Number	Number shows the H2 volume fraction
MEP	Mean Effective Pressure
ER	Equivalence Ratio
RPM	Revolution per minute
TDC	TOP Dead Centre
WOT	Wide Open Throttle

References

[1]Mehra, Roopesh Kumar, Hao Duan, Sijie Luo, Anas Rao, and Fanhua Ma. "Experimental and artificial neural network (ANN) study of hydrogen enriched compressed natural gas (HCNG) engine under various ignition timings and excess air ratios." Applied energy 228 (2018): 736-754.

[DOI: 10.22068/ase.2020.529]

[2]Hao, Duan, Roopesh Kumar Mehra, Sijie Luo, Zhibin Nie, Xiaohui Ren, and Ma Fanhua. "Experimental study of hydrogen enriched compressed natural gas (HCNG) engine and application of support vector machine (SVM) on prediction of engine performance at specific condition." International Journal of Hydrogen Energy (2019).

[3] Wallace JS, Cattelan AI. Hythane and CNG fueled engine exhaust emission comparison. Proceedings 10th World hydrogen Energy Conference, Cocoa Beach, USA, June 20–24, 1994. p. 1761–70.

[4] Raman V, Hansel J, Fulton J, Brudery D. Hythane, an ultraclean transport fuel. Proceedings, 10th World hydrogen Energy Conference, Cocoa Beach, USA, June 20–24, 1994. p. 1797–806.

[5] Hoekstra RL, Collier K, Mulligan N, Demonstration of hydrogen mixed gas vehicles, 10th World hydrogen Energy Conference, Cocoa Beach, USA, June 20–24, 1994.

[6] Hoekstra RL, Collier K, Mulligan N, Chew L. Experimental study of clean burning vehicle fuel. Int. J Hydrogen Energy 1995; 20:737–45.

[7] Paul, A.S., and James, S.W., 2005, "Effect of Hydrogen Content in Hydrogen Natural-Gas Fuel Mixtures on Emissions in a Lean-Burn IC Engine," ASME 2005 Fall Conference, pp. 363-371.

[8] Das LM. Utilization of hydrogen-CNG blend in internal combustion engine, 11th World Hydrogen Energy Conference, Stuttgart, Germany, and June 23–28, 1996. p. 1513–35.

[9] P.M. Dieguez ,J.C. Urroz. Marcelino-Sadaba, A.Perez-Ezcurdia, N.Benito-Amurrio, D. Sainz, L.M. Gandia." Experimental study of the performance and emission characteristics of an adapted commercial four-cylinder spark ignition engine running on hydrogen-methane mixtures." Applied energy , 2014 ;113: 1068-1076.

[10] Karim GA, Wierzba I, Al-Lousi Y. Methane–hydrogen mixtures as fuels. Int J Hydrogen Energy 1996; 20:625–31.

[11]Lim G, Lee S, Park C, Choi Y, Kim C. Effect of ignition timing retard strategy on NOx reduction in hydrogen-compressed natural gas blend engine with increased compression ratio. Int J Hydrogen energy 2014; 39:2399-2408.

[12] Das LM, Gulati R, Gupta PK. A comparative evaluation of the performance characteristics of a spark ignition engine using hydrogen and compressed natural gas as alternative fuels. Int J Hydrogen Energy 2000; 25:783–93.

[13] Shudo T, Shimamura K, Nakajima Y. Combustion and emissions in a methane DI strati1ed charge engine with hydrogen pre-mixing. JSAE Rev2000; 21:3 –7.

[14] Bauer CG, Forest TW. Effect of hydrogen addition on performance of methane-fueled vehicles. Part I: eDect on S.I. engine performance. Int J Hydrogen Energy 2001; 26:55–70.

[15] Paul, A.S., and James, S.W., 2005, "Effect of Hydrogen Content in Hydrogen Natural-Gas FuelMixtures on Emissions in a Lean-Burn IC Engine," ASME 2005 Fall Conference, pp. 363-371.

[16]Shrestha, B.S.O., Karim, G.A., 1999, "Hydrogen as an Additive to Methane for Spark Ignition Engine Applications," International Journal of Hydrogen Energy, Vol. 24, No. 6, pp. 577-586.

[17] Heffel, J. A., 2003, "NOX Emission and Performance Data for a Hydrogen Fueled Internal Combustion Engine at 1500 rpm using Exhaust Gas Recirculation," International Journal of Hydrogen Energy, Vol. 28, pp. 901-08.

[18]Bakul VYGCEJ, Xianming L. Computational fluid dynamics in industrial combustion. New York:CRC Press;2001.

[19]Hanjalic K.,popovac M.,Hadziabdic M. (2004). A robust Near-wall Elliptic-Relaxation Eddy- Viscosity turbulence model for CFD, In: international journal of heat an fluid flow, vol.25 , pp. 1047-1051.

[DOI: 10.22068/ase.2020.529]

[20] popovac M., Hanjalic K(2007).compound wall treatment for RANS Computation of complex Turbulent Flows and Heat Transfer, In: Flow, Turbulence, and combustion,Vol.78,pp.177-202.
[21]Basara B. (2006). An Eddy Viscosity Transport Model Based on Elliptic Relaxation Approachm In : AIAA Journal , Vol.44, pp.1686-1690
[22] Colin. O, Benkenida. A and Angelberger. C. a 3d Modeling of Mixing, Ignition and Combustion Phenomena in Highly Stratified Gasoline Engines- Oil and Gas Science and Technology, Rev. IFP, 58 1 (2003) 47-62

[DOI: 10.22068/ase.2020.529]